COMPARISONS OF THE NOAA-11 SBUV/2, UARS SOLSTICE, AND UARS SUSIM Mg II SOLAR ACTIVITY PROXY INDEXES*

RICHARD P. CEBULA and MATTHEW T. DELAND
Hughes STX Corporation, Lanham, MD 20706, U.S.A.

(Received 11 October, 1996; accepted 4 March, 1997)

Abstract. A NOAA-11 SBUV/2 Mg II solar activity proxy index has been created for the period February 1989 through October 1994 from the daily discrete mode solar irradiance data using an algorithm that utilizes a thorough instrument characterization. This product represents a significant improvement over the previously released NOAA-11 SBUV/2 sweep mode-based Mg II data set. As measured by the NOAA-11 Mg II index, the amplitude of solar rotational activity declined from approximately 4–7% peak-to-peak near the maximum of solar cycle 22 in 1989–1991 to roughly 1% peak-to-peak by late-1994. Corresponding to this decrease, the 27-day averaged NOAA-11 Mg II index decreased by 5.8% over this period. The NOAA-11 Mg II data set is compared with coincident data sets from the UARS SOLSTICE and SUSIM instruments. The impact of differences in instrument resolution and observation platform are examined with respect to both the absolute value and temporal variations of the Mg II index. Periodograms of the three indexes demonstrate comparable solar variation tracking. Between October 1991 and October 1994 predominate power occurs near 27 days, with secondary maxima in the power spectra near 29 and 25 days. Overall, there is low power near 13.5 days during this period. Dynamic power spectral analysis reveals the quasi-periodic and quasi-stationary nature of the middle UV variations tracked by the Mg II index, and periods of significant power near 13.5 days in mid-1991 and late-1994 through mid-1995.

1. Introduction

Variations in middle ultraviolet (UV, approximately 200–350 nm) solar irradiance are the primary driver of stratospheric ozone variations. Recent work indicates a 1.5–2% solar cycle variation of global mean total ozone (Stolarski *et al.*, 1991; Chandra and McPeters, 1994; Reinsel *et al.*, 1994) as well as solar cycle-driven variations in lower stratospheric temperature and geopotential height (McCormack and Hood, 1996; Hood, 1997). Tracking solar change in the photochemically important region of the spectrum near 200 nm to an accuracy of approximately 1% over a solar cycle is required to thoroughly understand the role of solar variations on atmospheric change (L. Hood, private communication, 1997). While several measurement programs are underway to measure solar cycle length UV irradiance variations (e.g., Cebula *et al.*, 1996; Woods *et al.*, 1996; Weber, Burrows, and Cebula, 1998), as a consequence of the difficulty of precisely tracking long-term instrument response changes, the 1% accuracy goal has yet to be met.

In lieu of direct solar UV measurements of sufficient accuracy, proxy indexes have been used to represent solar change. The core-to-wing irradiance ratio of the

* Paper presented at the SOLERS22 International Workshop, held at the National Solar Observatory, Sacramento Peak, Sunspot, New Mexico, U.S.A., June 17–21, 1996.

Solar Physics **177:** 117–132, 1998.

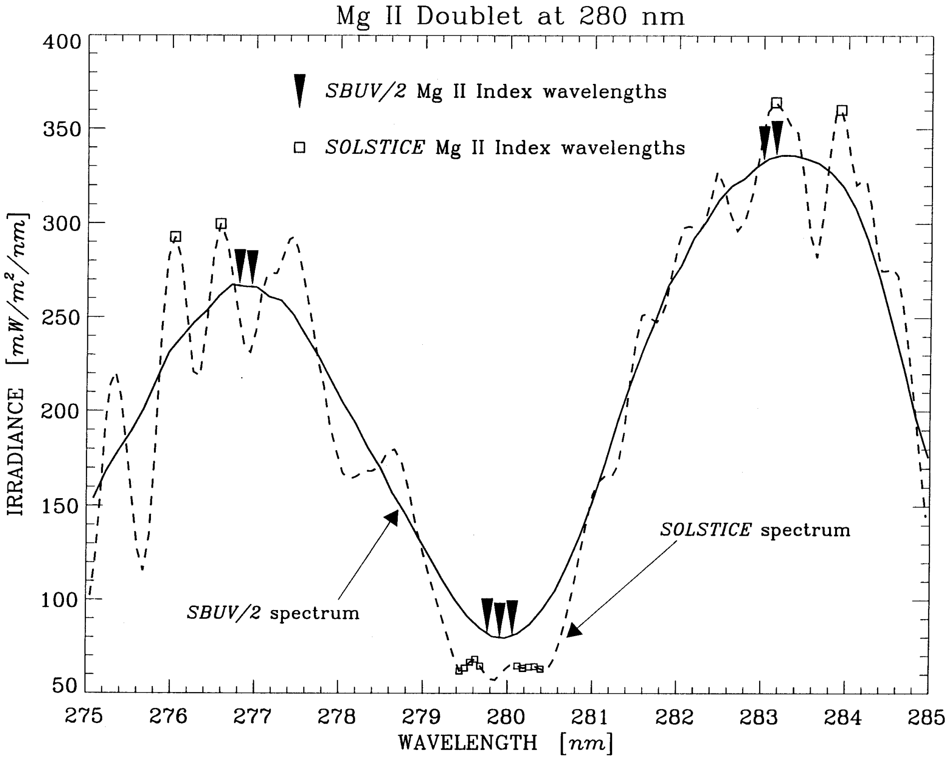

Figure 1. The Mg II doublet at 280 nm as observed by the NOAA-11 SBUV/2 instrument at 1.1 nm resolution (solid line) and the UARS SOLSTICE instrument at 0.24 nm resolution (dashed line). Positions of the 7 wavelengths used to construct the SBUV/2 classical discrete-mode Mg II index, Mg $\text{II}_{\text{NOAA-11}}$, are indicated by the arrows. The wavelengths used to construct Mg II_{SUSIM} (not shown) are very similar to those used to construct Mg $\text{II}_{\text{NOAA-11}}$. Positions of the wavelengths used to construct Mg $\text{II}_{\text{SOLSTICE}}$ are indicated by the small boxes.

Mg II 280 nm absorption feature, commonly known as the Mg II index, is a valuable tool for tracking solar UV activity (e.g., Heath and Schlesinger, 1986; Donnelly, 1988, 1991; Cebula, DeLand, and Schlesinger, 1992; DeLand and Cebula, 1993). A typical solar spectrum observed by the NOAA-11 SBUV/2 instrument near the Mg II feature is shown as the solid line in Figure 1. The use of an irradiance ratio cancels out most long-term instrument sensitivity changes which otherwise complicate solar UV irradiance measurements, and the construction of a ratio with evenly spaced wings removes any spectrally dependent changes which are approximately linear over the small wavelength interval used ($\Delta\lambda \sim 7$ nm). Mg II index variations can be coupled with spectral scaling factors to estimate solar irradiance variability in the 170–400 nm wavelength region (Cebula, DeLand, and Schlesinger, 1992; Lean *et al.*, 1992; DeLand and Cebula, 1993), which is important for understanding stratospheric photochemistry.

The initial Mg II index data set from the Nimbus-7 SBUV instrument began in November 1978, using 1.1 nm resolution sweep mode solar data. In this mode the instrument scanned the solar spectrum from approximately 160 to 400 nm. These measurements were continued by the NOAA-9 and NOAA-11 SBUV/2 instruments, with sweep mode (scanning approximately 160 to 405 nm) data beginning in March 1985 and December 1988, respectively. A composite Mg II index data set combining these three data sets was produced for the period November 1978 to May 1993, and distributed to the user community (DeLand and Cebula, 1993). This data set was designed to provide consistency with the Heath and Schlesinger (1986) Nimbus-7 SBUV Mg II index by using the spectral scan Mg II data from NOAA-9 and NOAA-11. The SBUV/2 instruments also use a discrete operating mode to observe the Mg II feature at 12 selected wavelengths with improved signal-to-noise characteristics and superior long-term wavelength stability (Donnelly, 1988; DeLand and Cebula, 1994). The NOAA-11 discrete mode Mg II solar data, which are available from February 1989 to October 1994, have recently been processed with an updated absolute calibration and a thorough long-term instrument characterization.

In this paper we present the NOAA-11 discrete-mode Mg II data set and compare it with the previously released sweep-mode-based Mg II data set (the NOAA-9 SBUV/2 Mg II data set is presented in a companion paper (DeLand and Cebula, 1998)). We also compare the NOAA-11 data with coincident Mg II data from the UARS SUSIM and UARS SOLSTICE instruments for the period September 1991 to October 1994. This provides an opportunity for a detailed examination of the impact of differences in both instrument resolution and observation platform on the absolute value and temporal variations of the Mg II index. The robustness of the solar variability information contained in the Mg II index is examined through statistical analysis of the three data sets. Our approach is complementary to that of de Toma *et al.* (1997), who focus on the degree to which the higher resolution SOLSTICE data reproduce the results of the lower resolution SBUV/2 instruments.

2. NOAA-11 Mg II Classical Discrete-Mode Proxy Index

The initial NOAA-11 SBUV/2 Mg II proxy index used in DeLand and Cebula (1993) was based on sweep-mode data in order to provide continuity with the Nimbus-7 SBUV and NOAA-9 SBUV/2 data sets also used in that paper. However, a Mg II proxy index based on SBUV/2 sweep mode data has a relatively poor signal-to-noise ratio (SNR) in comparison to the SNR of the Nimbus-7 SBUV Mg II index. This is because the SBUV/2 instruments measure the Mg II feature's wing irradiances at low count rate on the least sensitive radiometric range of the instrument, and electronic noise lowers the SNR (Schlesinger *et al.*, 1990). In addition, the NOAA-11 instrument's sweep-mode wavelength scale drifted by approximately 0.15 nm between 1989 and 1994, introducing an approximate 3%

time-dependent drift in the sweep-mode Mg II index. Daily NOAA-11 discrete-mode Mg II observations commenced in February 1989. An index constructed from these data has a much higher SNR than the sweep-mode index, not only because of a factor of 12.5 increase in the integration time, but also because limiting the wavelength interval scanned to the Mg II feature's region increases the number of scans per day by a factor of 4–5 over the number obtained in the sweep mode (DeLand and Cebula, 19 94). Further, the NOAA-11 SBUV/2 instrument's wavelength calibration stability was an order of magnitude better in discrete mode than in sweep mode (Ahmad *et al.*, 1994). Using a subset of the discrete-mode data and a less rigorous instrument characterization, Donnelly (1991) has constructed a modified discrete-mode Mg II index from the NOAA-9 SBUV/2 instrument's data. That index was constructed to circumvent some of the limitations of the preliminary instrument characterization, with the result that it was less sensitive to solar variations than is the sweep mode index. DeLand and Cebula (1994) suggested that an analogous classical discrete-mode Mg II index, constructed from discrete-mode measurements taken at essentially the same wavelengths as were used for the Nimbus-7 SBUV Mg II index, and employing a full instrument characterization, could combine the best features of the existing SBUV/2 proxy indexes.

The NOAA-11 SBUV/2 diffuser deployment mechanism failed on 16 October 1994, ending solar measurements, but permitting the continuation of daily ozone measurements. Following the launch of the NOAA-14 spacecraft on 30 December, 1994, the NOAA-11 spacecraft was deactivated on 10 April 1995, terminating NOAA-11 SBUV/2 observations. The NASA Goddard Space Flight Center's Ozone Processing Team has recently completed a meticulous instrument characterization for the entire NOAA-11 SBUV/2 data record (Hilsenrath *et al.*, 1996). Using that characterization, we have processed the discrete Mg II data set and produced a classical discrete-mode NOAA-11 SBUV/2 Mg II index (hereafter Mg $\text{II}_{\text{NOAA-11}}$). The most significant revisions to the processing algorithm are updates to the instrument's goniometry, photomultiplier tube detector gain, and corrections for small discrete-mode wavelength selection errors. The Mg $\text{II}_{\text{NOAA-11}}$ proxy index is presented in Figure 2(a). The solar rotational activity, as determined by approximate 27-day variations in Mg $\text{II}_{\text{NOAA-11}}$, declined from roughly 4–7% peak-to-peak near the maximum of solar cycle 22 in 1989–1991 to approximately 1% peak-to-peak after mid-1994. Note that the strength of the rotational modulation varies significantly from one rotation to next. Shown as the heavy solid line in Figure 2(a) is a 27-day running average of Mg $\text{II}_{\text{NOAA-11}}$, which removes the rotational modulation and shows long-term variations. From this curve it is seen that the mean level of solar activity, as measured by Mg $\text{II}_{\text{NOAA-11}}$, decreased by approximately 5.8% over this period.

The percent difference between the composite sweep-mode-based index (DeLand and Cebula, 1993) and Mg $\text{II}_{\text{NOAA-11}}$ is presented in Figure 3. During the period of overlap, 1989–1993, the composite index was based on NOAA-11 data. The day-to-day differences are predominately the result of noise in the sweep-mode Mg II

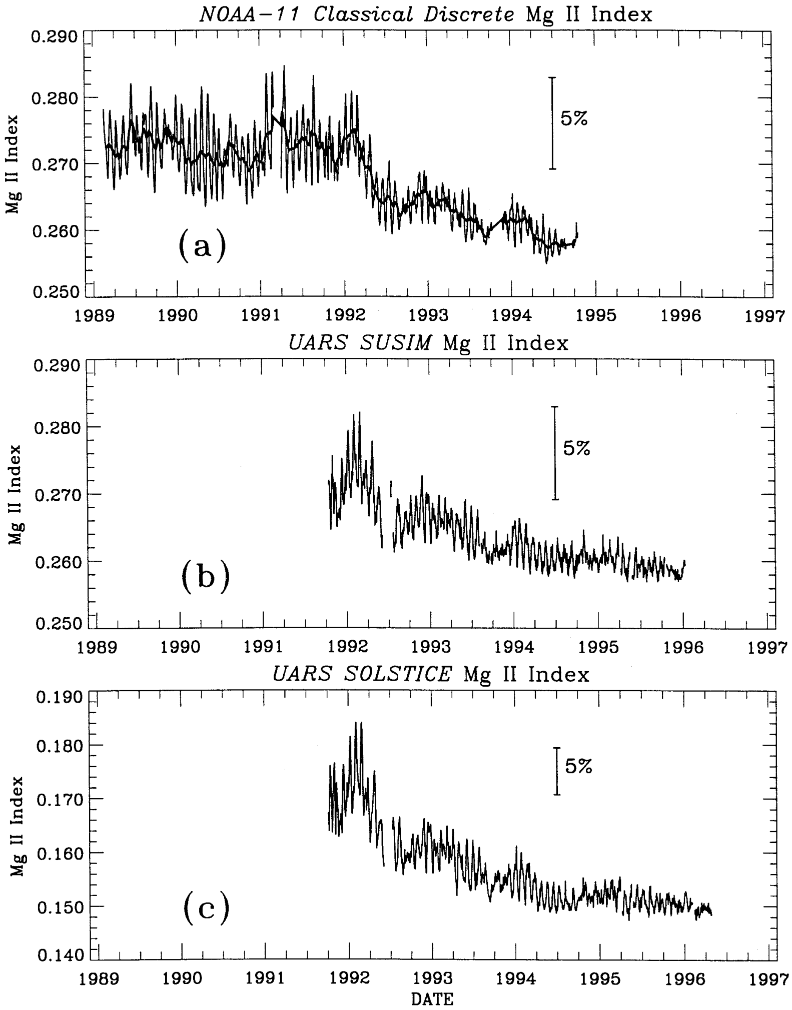

Figure 2. Time series of Mg II proxy index products from three instruments: (a) the NOAA-11 SBUV/2 classical discrete-mode Mg II index, Mg II$_{\mathrm{NOAA\text{-}11}}$; (b) the UARS SUSIM V18 Mg II index, Mg II$_{\mathrm{SOLSTICE}}$; (c) the UARS SOLSTICE V9 Mg II index, Mg II$_{\mathrm{SOLSTICE}}$. The heavy line in (a) is a 27-day running mean of Mg II$_{\mathrm{NOAA\text{-}11}}$.

data, resulting from the SNR and sampling limitations previously discussed. In addition, absolute and time-dependent differences are seen in Figure 3. The absolute difference is primarily the result of the procedure used to create the composite index. As discussed in DeLand and Cebula (1993), both the NOAA-11 SBUV/2 and the Nimbus-7 SBUV Mg II indexes were normalized to the NOAA-9 SBUV/2 Mg II index during their respective overlap periods. Due to small differences in the exact wavelengths used from one instrument to the next, as well as small but nontrivial inter-instrument differences in bandpass and slit function, the absolute value

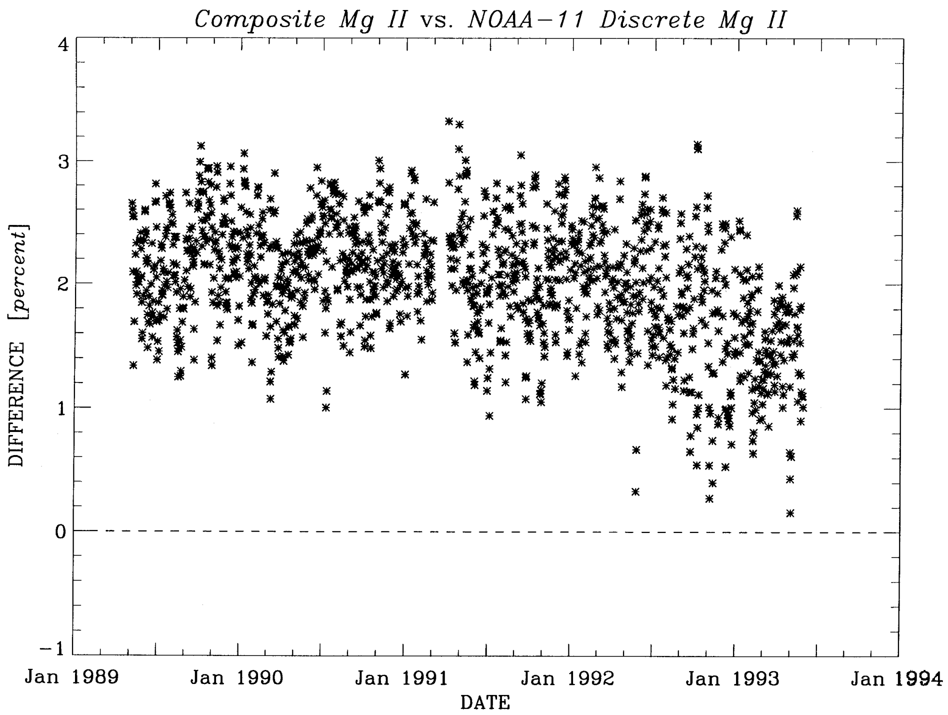

Figure 3. Percent difference between the SBUV-SBUV/2 composite Mg II index (DeLand and Cebula, 1993) and Mg $\text{II}_{\text{NOAA-11}}$. For the period shown here the composite index was based on NOAA-11 SBUV/2 sweep-mode data.

of each instrument's Mg II index and the instrument's sensitivity to solar change is unique (Hall and Anderson, 1988). Further, a long-term drift in the NOAA-9 instrument's wavelength calibration resulted in a 1% bias in its sweep-mode Mg II index in 1989 relative to 1985. These effects explain the absolute difference between the composite index and Mg $\text{II}_{\text{NOAA-11}}$ shown in Figure 3. The minor drift between the sweep-mode composite index and Mg $\text{II}_{\text{NOAA-11}}$ results from uncorrected drift in the NOAA-11 SBUV/2 instrument's sweep-mode wavelength calibration (DeLand and Cebula, 1994), and, to a lesser extent, revisions to other components of the absolute and long-term instrument characterizations.

3. Comparison to UARS SOLSTICE and SUSIM Mg II Indexes

The later portion of the NOAA-11 SBUV/2 measurement period coincides with the availability of solar irradiance data from the SOLSTICE (Rottman, Woods, and Sparn, 1993) and SUSIM (Brueckner *et al.*, 1993) instruments onboard the UARS satellite. Both UARS instruments began taking data in October 1991. The SUSIM V18 Mg II proxy index data set extends through December 1995, and is based on daily spectral measurements taken at 1.1 nm resolution (Floyd *et al.*, 1998). The corresponding SOLSTICE V9 Mg II data set is constructed from spectral data taken at 0.24 nm resolution (de Toma *et al.*, 1997; White *et al.*, 1998). The two UARS data sets, Mg II_{SUSIM} and Mg II_{SUSIM}, are presented in Figures 2(b) and 2(c), respectively. Comparisons of the two UARS Mg II data sets to Mg $\text{II}_{\text{NOAA-11}}$ are presented in Figure 4. The Mg $\text{II}_{\text{NOAA-11}}$ and Mg II_{SUSIM} indexes are based on solar irradiance measurements taken at similar spectral resolution and are constructed using similarly spaced (although not identical) core and wing samples. Hence, Mg $\text{II}_{\text{NOAA-11}}$ and Mg II_{SUSIM} should have approximately the same absolute value as well as comparable sensitivity to solar variations. Figure 4(a) indicates that the ratio of the two Mg II indexes is nearly unity. However, there is roughly a 1.5% relative drift between the two indexes during the first seven months of overlap. After the SUSIM data were interrupted for roughly 1.5 months due to problems with the UARS solar arrays, there is little additional drift from mid 1992 to the end of the overlap in the data record in October 1994. Although late 1991 and early 1992 is a period of significant rotational modulation, the mean level of solar activity did not change substantially during this seven month period. Further, from early-1993 to late-1994, when UV solar activity, as measured by the two Mg II proxy indexes, decreased by 2.3%, the drift between the two indexes was less than 0.5%. Hence, the relative drift in the NOAA-11 and SUSIM indexes in late 1991 and early 1992 is most likely due to a systematic drift in one or both of the instruments' indexes rather than a difference in their response to solar variability. Since the comparison of the Mg $\text{II}_{\text{NOAA-11}}$ and Mg $\text{II}_{\text{SOLSTICE}}$ indexes presented in Figure 4(b) does not show a corresponding drift during this seven month period, we suspect there is an uncorrected systematic drift in the Mg II_{SUSIM} during the initial phase of that instrument's operation. Mg II_{SUSIM} exhibits a similar drift with respect to the NOAA-9 SBUV/2 Mg II data set, Mg $\text{II}_{\text{NOAA-9}}$ presented by DeLand and Cebula (1998). There is no relative drift between Mg $\text{II}_{\text{NOAA-9}}$ and Mg $\text{II}_{\text{NOAA-11}}$.

The relationship between Mg II_{SUSIM} and Mg $\text{II}_{\text{NOAA-11}}$ is further examined via the scatter plot and linear regression analysis presented in Figure 5(a) and Table I. While there is an approximately linear relationship between the two indexes for the entire period, the data for first seven months, denoted by the 'Xs' in Figure 5(a), clearly show more dispersion and an absolute offset relative to the data for the rest of the overlap period. The linear correlation coefficient for the period October 1991 –June 1992 is only 0.900, indicating that 20% of the variance in Mg II_{SUSIM} is not explained by the linear relation with respect to Mg $\text{II}_{\text{NOAA-11}}$. The linear correlation coefficient for the rest of the data record, July 1992–October 1994, is 0.954. Therefore, for this period about 91% of the variance in Mg II_{SUSIM} is explained by the linear relation with respect to Mg $\text{II}_{\text{NOAA-11}}$. The slope of the linear regression for the period July 1992 through October 1994 is 0.994, indicating that, as predicted, the two instruments have very similar responses to solar change. Note that the correlation coefficient is slightly greater for the entire period, October 1991–

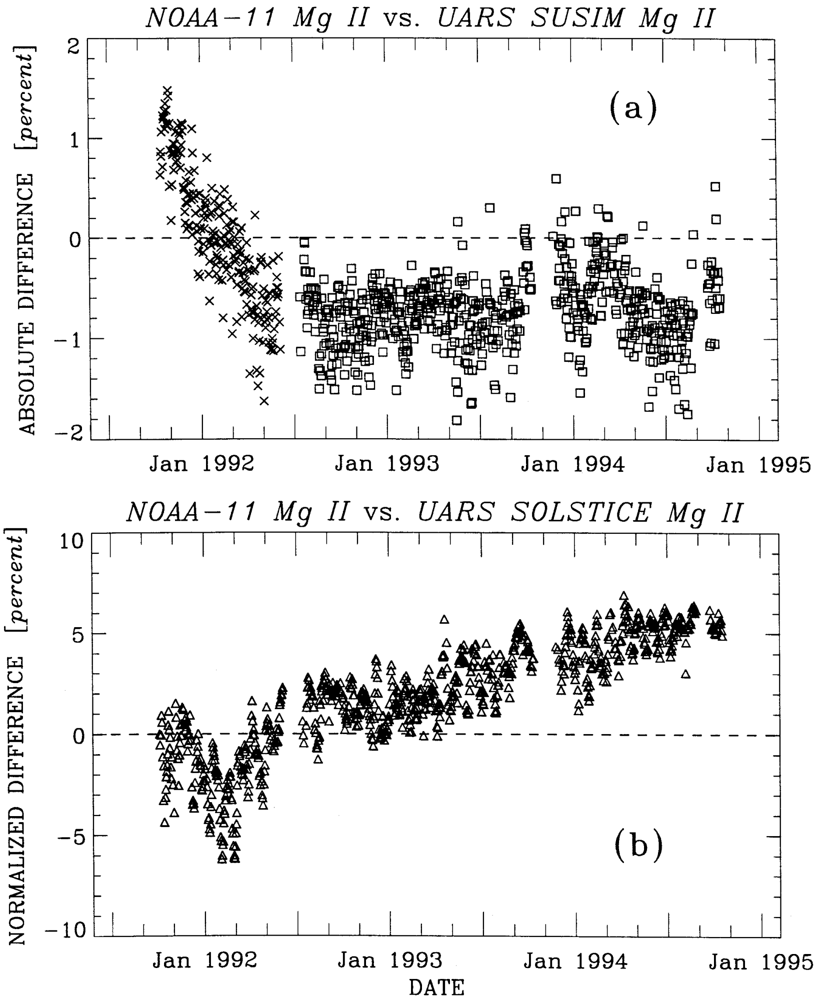

Figure 4. Percent differences between the time series of the two UARS Mg II indexes and Mg $\text{II}_{\text{NOAA-11}}$, for the period of common measurements, October 1991 through October 1994: (a) Mg II_{SUSIM}; (b) Mg $\text{II}_{\text{SOLSTICE}}$. The crosses in (a) correspond to data taken during the first seven months of SUSIM operations and the squares to data taken after this period. The SUSIM to SBUV/2 comparison is normalized by the absolute ratio of the two indexes. As discussed in the text, the change shown in (b) is physical in origin.

October 1994 ($r = 0.963$) than it is for the July 1992–October 1994 period, despite the inclusion of the early data with increased dispersion. This is a consequence of the regression procedure; whereas the latter period encompasses only about one-half the dynamic range of the solar cycle, the full dynamic range of the solar cycle is included in the former period. A similar, although significantly smaller effect is seen in the regression between Mg $\text{II}_{\text{SOLSTICE}}$ and Mg $\text{II}_{\text{NOAA-11}}$ discussed below. It is therefore beneficial and important to maximize the dynamic range of the data

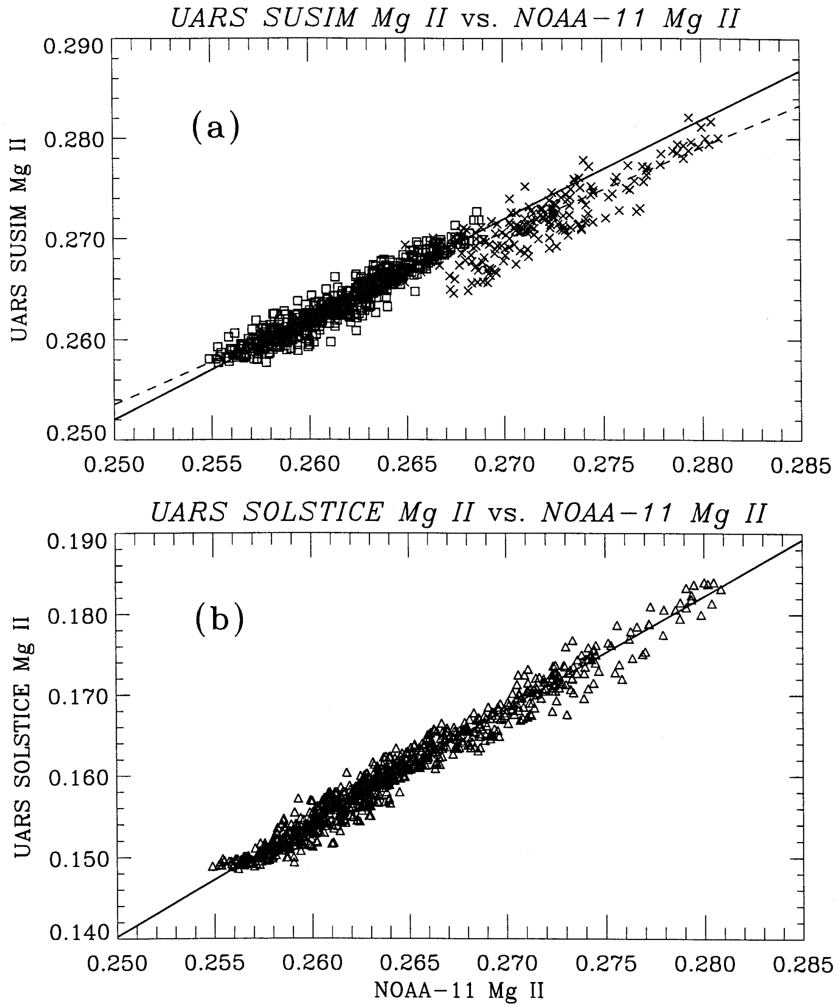

Figure 5. Comparisons of the two UARS Mg II indexes to Mg $\text{II}_{\text{NOAA-11}}$; (a) Mg II_{SUSIM}, and (b) Mg $\text{II}_{\text{SOLSTICE}}$. The crosses in (a) correspond to data taken during the first seven months of SUSIM operations and the squares to data taken after this period. The lines are the result of least-square linear regression fits. In (a) the dashed line is a fit to the period October 1991–October 1994 and the solid line is the fit to the period July 1992–October 1994. The solid line in (b) is the result of fitting the entire period of coincident measurements, October 1991–October 1994.

sets used in the linear regression analysis, provided that significant drifts have been removed. If the cause of the drift in Mg II_{SUSIM} can be identified and corrected, the relationship between Mg II_{SUSIM} and Mg $\text{II}_{\text{NOAA-11}}$ should be redetermined using the entire dynamic range of the solar cycle. Doing so will yield a more accurate and precise relationship than is currently achievable.

Interpretation of the comparison between Mg $\text{II}_{\text{SOLSTICE}}$ and Mg $\text{II}_{\text{NOAA-11}}$, presented in Figure 4(b), is more complicated than is the comparison between

Table I

Slope and linear correlation coefficients derived from least-squares linear regression comparisons of Mg $\text{II}_{\text{SOLSTICE}}$ and Mg II_{SUSIM} with Mg $\text{II}_{\text{NOAA-11}}$

Data set	Slope	Linear correlation coefficient
All SUSIM: Oct. 1991–Oct. 1994	0.852	0.963
SUSIM: Oct. 1991–June 1992	0.855	0.900
SUSIM: July 1992–Oct. 1994	0.994	0.954
All SOLSTICE: Oct. 1991–Oct. 1994	1.40	0.984
SOLSTICE: Oct. 1991–June 1992	1.31	0.958
SOLSTICE: July 1992–Oct. 1994	1.41	0.963

Mg $\text{II}_{\text{NOAA-11}}$ and Mg II_{SUSIM} as a result of differences in instrument resolution and processing algorithms. Figure 2 shows that the absolute value of Mg $\text{II}_{\text{SOLSTICE}}$ is approximately a factor of two smaller than are the absolute values of Mg $\text{II}_{\text{NOAA-11}}$ and Mg II_{SUSIM}. A typical scan of SOLSTICE $\sim$0.24 nm resolution solar spectral irradiance data in the vicinity of the Mg II absorption feature, shown as the dashed curve in Figure 1, is useful in understanding these differences. The higher spectral resolution data reveal significantly more spectral structure in the absorption feature than do the lower spectral resolution data. As observed by SOLSTICE the Mg II h and k emission lines are visible as distinct emission peaks in the core of the broad absorption feature. In contrast, these central emission peaks are not visible at the 1.1 nm resolution of the SBUV/2 and SUSIM instruments. Because of the higher resolution, the core of the Mg II feature as observed by SOLSTICE contains no contribution from the photospheric wing wavelengths (as opposed to the Mg II feature at 1.1 nm resolution, where the core contains a non-negligible photospheric content). Since the core of the Mg II feature as observed by SOLSTICE originates higher in the solar atmosphere at a correspondingly higher temperature than does the core of the feature when observed by NOAA-11, Mg $\text{II}_{\text{SOLSTICE}}$ and Mg $\text{II}_{\text{NOAA-11}}$ have different sensitivities to solar irradiance variations. Thus, except for the nonlinear behavior observed in early 1992, the change in the relative percent difference between the two indexes presented in Figure 4(b) is physical rather than instrumental in origin. Note that the temporal dependence of this feature is quite distinct from the drift between Mg II_{SUSIM} and Mg $\text{II}_{\text{NOAA-11}}$ shown in Figure 4(a). We thus suspect this feature may result from an transitory feature in Mg $\text{II}_{\text{SOLSTICE}}$. A scatter plot of Mg $\text{II}_{\text{SOLSTICE}}$ versus Mg $\text{II}_{\text{NOAA-11}}$ (Figure 5(b)) and linear regression analysis results (Table I) show that the two indexes are well correlated ($r = 0.984$) and scale approximately linearly. In contrast to the comparison between Mg II_{SUSIM} and Mg $\text{II}_{\text{NOAA-11}}$ presented previously, note that the linear regression coefficients for the October 1991–June 1992 ($r = 0.958$) and July 1992–October 1994 ($r = 0.963$) periods are nearly identical. The slope of this regression fit is 1.40, which is almost identical to the result obtained by de Toma *et al.* (1997) in their analysis of these data sets (their Equation (8) Mg $\textsc{ii}_{\text{NOAA-11}} = 0.153 + 0.696 \times$ Mg $\textsc{ii}_{\text{SOLSTICE}}$. As determined from the extreme values of Figure 5(b), the SOLSTICE index has approximately a factor of 2.2 greater response to rotational and solar cycle change than do the lower resolution indexes (SBUV/2 and SUSIM). This enhanced sensitivity, which is a consequence of SOLSTICE's higher spectral resolution, results in the change noted in Figure 4(b). de Toma *et al.* (1997) also degraded the SOLSTICE irradiance data to the nominal SBUV/2 resolution and recomputed Mg II index values. They found a slope of 0.927 when these data were regressed against Mg $\textsc{ii}_{\text{NOAA-11}}$. This indicates that, as observed in the Mg II feature, the higher resolution SOLSTICE irradiance data are more responsive to chromospheric activity, even when degraded to comparable resolution, than are the lower resolution SBUV/2 irradiance data. White *et al.* (1998) compared the effects of degrading the SOLSTICE data to the nominal SBUV/2 and SUSIM resolution. Consistent with the current work, White *et al.* (1998) found that the sensitivity of higher resolution data to both solar rotational and long-term modulation is approximately twice the sensitivity of the index when observed at 1.1 nm resolution. Scale factors derived from SBUV/2 data (DeLand and Cebula, 1993) must therefore be rescaled for use with Mg $\textsc{ii}_{\text{SOLSTICE}}$.

4. Power Spectral Analysis

Using the technique described by Horne and Baliunas (1986) and Lean and Brueckner (1989), we have constructed periodograms of Mg $\textsc{ii}_{\text{NOAA-11}}$, Mg $\textsc{ii}_{\text{SOLSTICE}}$, and Mg $\textsc{ii}_{\text{SUSIM}}$ for the period of coincident measurements, October 1991 to October 1994, to examine the power spectra of the three data sets. The periodograms, shown in Figure 6, demonstrate comparable solar variation tracking between the three indexes, consistent with the high correlation coefficients observed previously. For this period the predominant power occurs with a period near 27 days, with secondary maxima in the power spectra near 29 and 25 days. Overall, there is relatively low power near 13.5 days during the interval of coincident data. This indicates that, during this period, solar UV variability was dominated by a single active region at a time.

Shown in Figure 7 is the result of a dynamic power spectral analysis of the three Mg II data sets. The analysis was performed by fixing the periodogram data window at a width of 256 days and stepping through the data sets in 64-day increments, following the work of Bouwer (1992). This analysis reveals the complex quasi-periodic and quasi-stationary nature of middle UV solar variations. Note the significant changes in power surrounding the dominant 27-day periodicity, which explains the presence of the secondary maxima noted in Figure 6 near 29 and 25 days. Strong approximate 35-day and 30-day periodicities were observed by the NOAA-11 instrument during late 1989 and mid-1990, respectively. Mg $\textsc{ii}_{\text{NOAA-11}}$ also exhibits a period of approximate 13.5-day solar variability from the middle

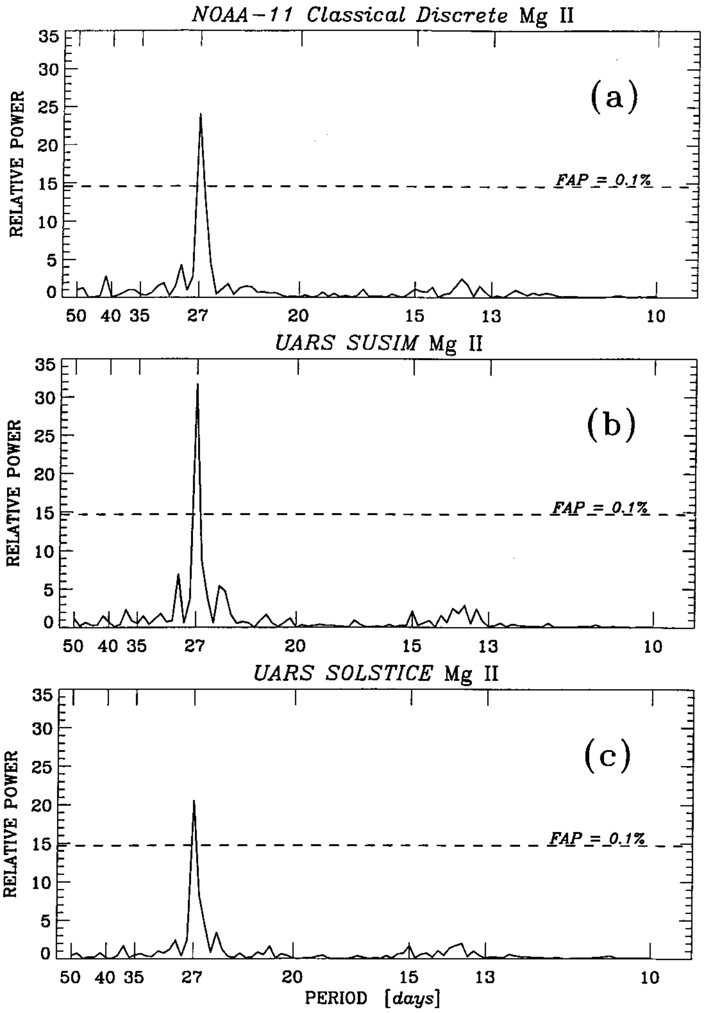

Figure 6. Periodogram analysis of the three Mg II data sets for the period October 1991–October 1994: (a) Mg $\text{II}_{\text{NOAA-11}}$; (b) Mg II_{SUSIM}; (c) Mg $\text{II}_{\text{SOLSTICE}}$. The dashed line indicates the false alarm probability (FAP) level of 0.1%; features with power above this FAP are statistically significant at the 99.9% confidence level (Horne and Baliunas, 1986).

of 1991 through early 1992, with the peak in the power occurring shortly after the UARS launch. This variability indicates the emergence of active regions on opposing faces of the Sun simultaneously. The very end of this episode of approximate 13.5-day periodicity is just barely visible at the beginning of the Mg $\text{II}_{\text{SOLSTICE}}$ data set. A period of relatively weak 13.5-day periodicity was observed by all three instruments in spring 1993. This period gives rise to the small peak near 13.5 days seen in Figure 6.

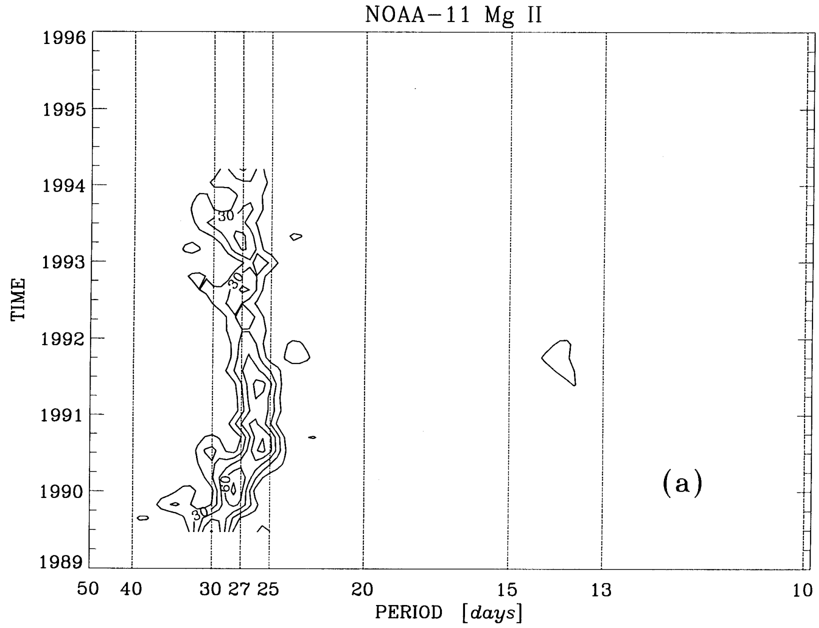

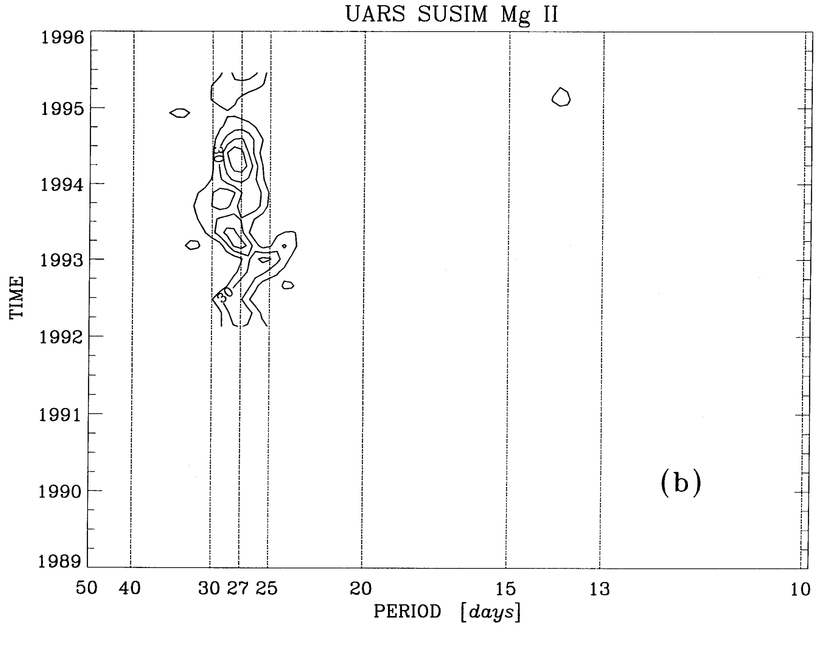

Figure 7a-c. Dynamic power spectral analysis of the three Mg II data sets: (a) Mg $\text{II}_{\text{NOAA-11}}$; (b) Mg II_{SUSIM}; (c) Mg $\text{II}_{\text{SOLSTICE}}$. Contour levels represent periodogram power in increments of 15, corresponding to the vertical scale of Figure 6. All contour levels shown are statistically significant at the 99.9% level.

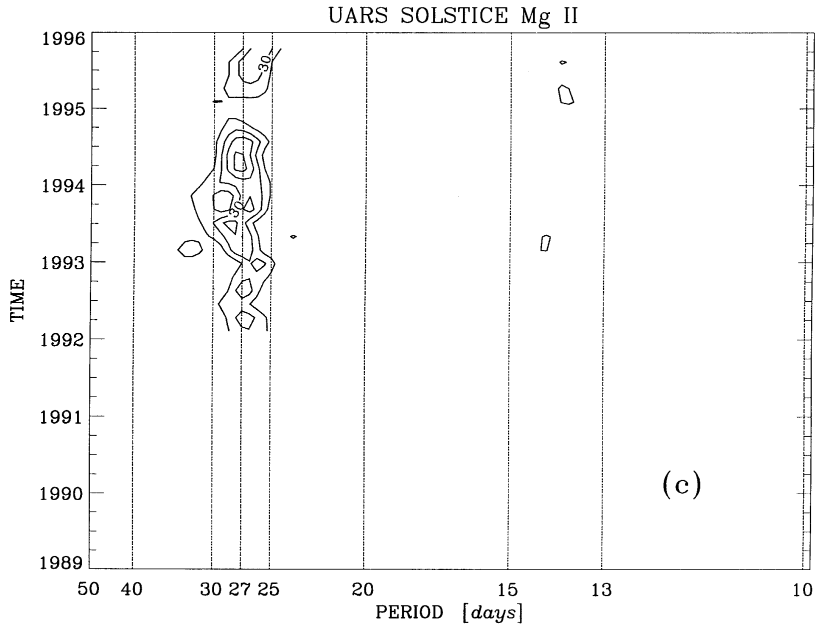

Figure 7. Continued.

An extended period of significant, approximate 13.5-day periodicity commenced in September 1994, shortly before the termination of the NOAA-11 SBUV/2 solar measurements. The analysis technique employed here, coupled with the termination of the NOAA-11 data set in mid October 1994, prohibits revelation of this change in solar activity in the dynamic power spectra of Mg $\text{II}_{\text{NOAA-11}}$. The Mg II_{SUSIM} and Mg $\text{II}_{\text{SOLSTICE}}$ dynamic power spectra (Figures 7(b) and 7(c), respectively) reveal the presence of this periodicity. As demonstrated in the periodogram analysis presented in Figure 6 of DeLand and Cebula (1998), the NOAA-9 SBUV/2 instrument also observed persistent approximate 13.5-day solar variability from September 1994 through March 1995. These observations are significant because this period of strong 13-day periodicity was observed near solar cycle 22 minimum. During the only other solar minimum period monitored to date in the UV, 1985–1986, very little 13.5-day activity was observed (Heath and Schlesinger, 1986). These observations, and the differences in activity seen during the maximum of solar cycle 22 versus that seen during cycle 21 maximum, suggest that each solar cycle is unique and that we are not yet at the point where one can simply use the middle UV solar data sets we presently have to extrapolate to the future.

5. Conclusions

A classical discrete-mode Mg II index, Mg $\text{II}_{\text{NOAA-11}}$ has been created from the entire six-year NOAA-11 SBUV/2 data set. This product has better signal-to-noise characteristics and long term accuracy than the sweep-mode NOAA-11 Mg II data set previously published by DeLand and Cebula (1993). Comparisons of Mg $\text{II}_{\text{NOAA-11}}$ with Mg $\text{II}_{\text{SOLSTICE}}$ and Mg II_{SUSIM} indicates that each instrument is capable of accurately tracking both short- and long-term solar variations. There is an approximate 1.5% relative drift between Mg II_{SUSIM} and Mg $\text{II}_{\text{NOAA-11}}$ during the first seven months of SUSIM operations which needs to be understood. No corresponding drift is seen between Mg $\text{II}_{\text{NOAA-11}}$ and either Mg $\text{II}_{\text{SOLSTICE}}$ or Mg $\text{II}_{\text{NOAA-9}}$. Mg $\text{II}_{\text{SOLSTICE}}$ and Mg $\text{II}_{\text{NOAA-11}}$ exhibit good linear correlation ($r = 0.984$) even though the SOLSTICE index has roughly a factor of 2.2 greater response to solar variations relative to the SBUV/2 index and Mg $\text{II}_{\text{SOLSTICE}}$ exhibits a transitory feature with respect to Mg $\text{II}_{\text{NOAA-11}}$ in early 1992, during the first year of SOLSTICE operation. The Mg $\text{II}_{\text{NOAA-11}}$ data are available from the authors (cebula@ssbuv.gsfc.nasa.gov). The Mg $\text{II}_{\text{NOAA-9}}$ data are also available from the authors for the period June 1986 through May 1996. In the near future these two data sets will be combined with the Nimbus-7 SBUV Mg II data to create a single Mg II proxy index covering the period November 1978 through May 1996.

Acknowledgements

The raw SBUV/2 data were provided by W. G. Planet and H. D. Bowman of NOAA. We thank L. Floyd and D. K. Prinz of NRL and G. de Toma of HAO for supplying the SUSIM and SOLSTICE Mg II indexes and for useful discussions. J. Lean provided the IDL software used for the periodogram analysis, as well as valuable advice on its use. This work was supported by NASA Grant NASW-4864.

References

Ahmad, Z., DeLand, M. T., Cebula, R. P., Weiss, H., Wellemeyer, C. G., Planet, W. G., Lienesch, J. H., Bowman, H. D., Miller, A. J., and Nagatani, R. M.: 1994, *J. Geophys. Res.* **99**, 22975.

Bouwer, S. D.: 1992, *Solar Phys.* **142**, 365.

Brueckner, G. E., Edlow, K. L., Floyd, L. E., Lean, J. L., and VanHoosier, M. E.: 1993, *J. Geophys. Res.* **98**, 10695.

Cebula, R. P., DeLand., M. T., and Schlesinger, B. M.: 1992, *J. Geophys. Res.* **97**, 11 613.

Cebula, R. P., Thuillier, G. O., VanHoosier, M. E., Hilsenrath, E., Herse, M., Brueckner, G. E., and Simon, P. C.: 1996, *Geophys. Res. Letters* **23**, 2289.

Chandra, S., and McPeters, R. D.: 1994, *J. Geophys. Res.* **99**, 20 665.

DeLand, M. T. and Cebula, R. P.: 1993, *J. Geophys. Res.* **98**, 12 809.

DeLand, M. T. and Cebula, R. P.: 1994, *Solar Phys.* **152**, 61.

DeLand, M. T. and Cebula. R. P.: 1998, *Solar Phys.* **177**, 105 (this issue).

de Toma, G., White, O. R., Knapp, B. G., Rottman, G. J., and Woods, T. N.: 1997, *J. Geophys. Res.* **102**, 2597.

Donnelly, R. F.: 1988, *Adv. Space Res.* **8** (7), 77.
Donnelly, R. F.: 1991, *J. Geomag. Geoelectr. Suppl.* **43**, 835.
Floyd, L., Reiser, P., Crane, P., Herring, L, Prinz, D., and Brueckner, G.: 1998, *Solar Phys.* **177**, 105 (this issue).
Hall. L. A., and Anderson, G. P.: 1988, *Ann. Geophys.* **6**, 531.
Heath, D. F. and Schlesinger, B. M.: 1986, *J. Geophys. Res.* **91**, 8672.
Hilsenrath, E. *et al.*: 1996, *EOS Trans. Amer. Geophys. Union, Fall Meet. Suppl.* **77** (46), F62.
Horne. J. H. and Baliunas, S. L.: 1986, *Astrophys. J.* **302**, 757.
Hood, L. L.: 1997, *J. Geophys. Res.* **102**, 1355.
Lean J. L., and Brueckner, G. E.: 1989, *Astrophys. J.* **337**, 568.
Lean, J., VanHoosier, M., Brueckner, G., Prinz, D., Floyd, L., and Edlow, K.: 1992, *Geophys. Res. Letters* **19**, 2203.
McCormack, J. P. and Hood, L. L.: 1996, *J. Geophys. Res.* **101**, 20933.
Reinsel. G. C. *et al.*: 1994, *J. Geophys. Res.* **99**, 5449.
Rottman, G. J., Woods, T. N., and Sparn, T. P.: 1993, *J. Geophys. Res.* **98**, 10 667.
Schlesinger, B. M., Cebula, R. P., Heath, D. F., DeLand, M. T., and Hudson, R. D.: 1990, in K. H. Schatten and A. Arking (eds.), *Climate Impact of Solar Variability*, NASA Conf. Publ. 3086, p. 341.
Stolarski. R. S.. Bloomfield, P., McPeters, R. D., and Herman, J. R.: 1991, *Geophys. Res. Letters* **18**, 1015.
Weber, M., Burrows, J. P., and Cebula, R. P.: 1998, *Solar Phys.* **177**, 63 (this issue).
White, O. R., de Toma, G., Rottman, G. J., Woods, T. N., and Knapp, B. G.: 1998, *Solar Phys.* **177**, 89 (this issue).
Woods. T. N. *et al.*: 1996, *J. Geophys. Res.* **101**, 9541.